Highlights of Spanish Astrophysics XII, Proceedings of the XVI Scientific Meeting of the Spanish Astronomical Society held on July 15 - 19, 2024, in Granada, Spain. M. Manteiga, F. González Galindo, A. Labiano Ortega, M. Martínez González, N. Rea, M. Romero Gómez, A. Ulla Miguel, G. Yepes, C. Rodríguez López, A. Gómez García and C. Dafonte (eds.), 2025

Multi-scale study of sulphur chemistry in hot corinos: characterising the envelope of Class 0 protostars

Fernández-Ruiz, P.[1], Fuente, A.[1], and Esplugues, G.[2]

[1] Centro de Astrobiología (CAB), CSIC-INTA, Carretera de Ajalvir Km. 4, Torrejón de Ardoz, 28850 Madrid, Spain
[2] Observatorio Astronómico Nacional (OAN), Alfonso XII 3, 28014 Madrid, Spain

Abstract

Due to the high dust temperature, ices in hot corinos are sublimated and all the volatile sulphur is expected to return to the gas phase. Our goal is to determine the amount of gaseous sulphur as well as the chemical composition of the sulphur budget in the envelopes of these warm objects. We have observed Class 0 protostars HH 212 and NGC 1333 IRAS4A, which are known to harbor hot corinos, in the spectral ranges $\lambda = 7$, 3, 2 and 1 mm. We search for transitions of 25 S-bearing species and perform rotational diagrams to find their column densities, rotational temperatures and abundances.

1 Introduction

When the prestellar core of a future low-mass protostar progressively collapses and heats the infalling envelope, a region of compact (< 100 au), hot (> 100 K) and dense ($> 10^7$ cm^{-3}) dust and gas appears. These regions are known as hot corinos, and they present a very rich chemistry [3, 4] with dozens of complex organic molecules (COMs) detected [7]. Therefore, studying the chemistry of hot corinos is key to understand the overall star and planet formation processes. It is specially interesting to evaluate the differences in their chemistry through their evolution, as well as the role that the environment plays in them.

While sulphur is an important element that takes part in the development of biological systems on Earth [9], we only account for a fraction of the total cosmic abundance of sulphur in dense molecular gas [12]. It has been proposed that this element might be locked into a semirefractory material such as S_8 [11], but this is still not confirmed by observations. For this reason, we are focusing on the chemistry of sulphur bearing species found in hot corinos, confident it can shed some light on the problem of the missing sulphur as well as show how the chemical composition of the sulphur budget evolves during the star formation process.

In this work, we explore the chemistry of two Class 0 protostars that are known to have hot corinos: HH 212 and NGC 1333 IRAS4A. These objects are part of the ECHOS project [5] (PI: G. Esplugues) sample (see Table 1), in which we have low-mass protostars along different evolutionary stages and surrounded by different environments. An analysis of object B 335 from the sample was already done in [5].

Table 1: ECHOS project sample of low-mass protostars.

Source	Cloud	Coordinates RA (J2000)	 Dec (J2000)	Distance (pc)	Comment
B 335	Isolated	19:37:00.9	+07:34:09.9	100	Class 0
HH 212	Orion	05:43:51.4	−01:02:53.1	414	Class 0
NGC 1333 IRAS4A	Perseus	03:29:10.5	+31:13:30.9	312	Class 0
SVS13-A	Perseus	03:29:03.7	+31:16:03.8	312	Class I

2 Observations

The observations were carried out by Yebes 40m and IRAM 30m telescopes in the frame of projects ECHOS and ASAI [8] (PIs: B. Lefloch & R. Bachiller), and the data was reduced using CLASS and GREG from the GILDAS software[1]. Yebes 40m covered the 31.0–50.3 GHz Q-band, while IRAM 30m covered the 73–118 GHz and 130–175 GHz spectral ranges for HH 212 and B 335, and an additional 200-276 GHz range for IRAS4A. Antenna temperatures were converted to main beam brightness temperatures using parameters in [5].

3 Data Analysis & Results

We have searched for all possible transitions of 25 sulphur bearing molecules in our observed spectra for both HH 212 and IRAS4A. To complete our molecule survey we also added four non-sulphur bearing species: $C^{17}O$, $C^{18}O$, H_2CO and CH_3OH. These molecules were not studied in [5] so, to allow a comparison between all three objects, we analysed those in B 335 as well. Detected lines, with rms above 3σ, were fitted by a Gaussian to obtain its velocity integrated intensity. Some of the lines also had a wide outflow component, therefore a secondary Gaussian fit was needed. This was the case for many IRAS4A molecules (CS, $C^{34}S$, ^{13}CS, OCS, HCS^+, SO, H_2CS, SO_2, H_2S, CH_3OH and H_2CO), a transition of SO in HH 212 and a few transitions of CH_3OH in B 335. We will be focusing on the narrow component for the length of this work.

---

[1] http://www.iram.fr/IRAMFR/GILDAS.

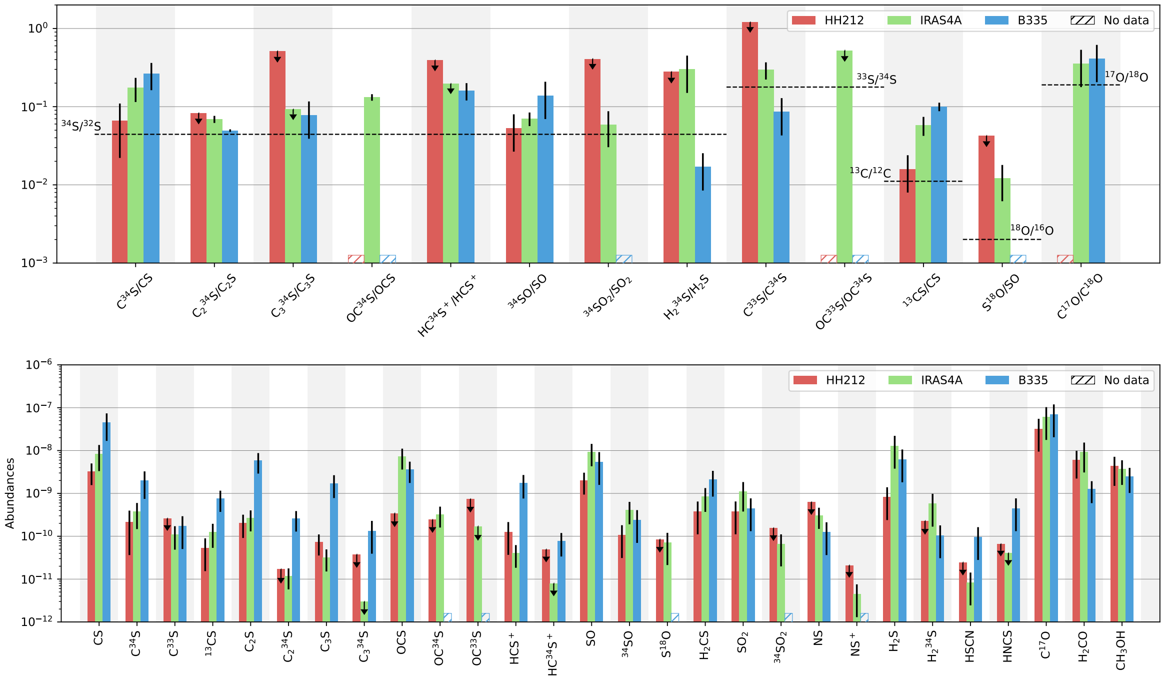

Figure 1: Top: isotopologue ratios of molecules in objects HH 212, IRAS4A and B 335, along with dash lines that represent their corresponding solar isotopic ratio [2]. Bottom: abundances of each species in objects HH 212, IRAS4A and B 335.

3.1 Rotational diagrams & Column densities

For each molecule with two or more transitions, we have computed its rotational temperature ($T_{\rm rot}$) and column density (N) using the method in [6]. The results obtained with this method are in Table 2, along with the errors derived from the linear fitting and the results of B 335 from [5]. We can observe that a few species (CS, C^{34}S, ^{13}CS, OCS, H$_2$CS, SO$_2$, CH$_3$OH and H$_2$CO in IRAS4A; C$_2$S and CH$_3$OH in B 335) also had a second slope with warmer $T_{\rm rot}$ in the diagram, which might mean that the molecule is also tracing an inner region of the protostar, as opposed to only the outer envelope. Some species had an anomalously high temperature ($T_{\rm rot} > 30$ K) in their colder slope as well (C$_3$S in HH 212; OCS, OC^{34}S, H$_2$S and H$_2$^{34}S in IRAS4A), which makes them perfect candidates to potentially trace the hot corino of each object. Further research needs to be conducted using interferometric observations and chemical models to confirm this.

To compute the column density of species where only one transition was found we must assume a rotational temperature, indicated in Table 2. Taking into account an adequate temperature for each molecule, we get the results in Table 2, with a 50% error. For undetected molecules we can also obtain a column density upper limit by assuming the temperature and that the integrated intensity must be under 3σ. We used the lowest upper energy transition of each molecule in our spectra for these and the results can be found in Table 2 as well.

Table 2: Column densities and rotational temperatures for the narrow component of each molecule in sources HH 212, IRAS4A and B 335.

	HH 212		IRAS4A		B 335[a]	
Species	N (cm^{-2})	$T_{\rm rot}$ (K)	N (cm^{-2})	$T_{\rm rot}$ (K)	N (cm^{-2})	$T_{\rm rot}$ (K)
CS	$(8.0\pm1.3)\times10^{12}$	5.0 ± 0.4	$(2.8\pm1.3)\times10^{13}$	5.8 ± 1.7	$(8.0\pm2.0)\times10^{13}$	3.6 ± 0.8
			$(1.8\pm0.9)\times10^{13}$	16.7 ± 8.3		
$C^{34}S$	$(5.3\pm3.5)\times10^{11}$	2.8 ± 0.7	$(5.1\pm1.7)\times10^{12}$	4.5 ± 0.9	$(2.1\pm0.8)\times10^{13}$	2.7 ± 0.7
			$(2.8\pm1.4)\times10^{12}$	10.2 ± 5.1		
$C^{33}S$	$< 6.4\times10^{11}$ [b]	5.0[c]	$(1.9\pm0.5)\times10^{12}$	11.0 ± 1.6	$(1.8\pm0.9)\times10^{12}$	2.9 ± 0.5
^{13}CS	$(1.3\pm0.6)\times10^{11}$	4.7 ± 2.3	$(1.59\pm0.03)\times10^{12}$	6.5 ± 0.1	$(8.0\pm1.0)\times10^{12}$	2.8 ± 0.9
			$(1.2\pm0.6)\times10^{12}$	20.7 ± 10.4		
C_2S	$(5.0\pm1.2)\times10^{11}$	5.7 ± 0.6	$(3.0\pm0.5)\times10^{12}$	13.3 ± 0.8	$(5.4\pm0.8)\times10^{13}$	5.0 ± 0.5
					$(1.9\pm0.6)\times10^{12}$	15.0 ± 1.0
$C_2{}^{34}S$	$< 4.2\times10^{10}$ [b]	5.7[c]	$(2.1\pm0.2)\times10^{11}$	20.7 ± 1.9	$(2.7\pm0.1)\times10^{12}$	6.4 ± 0.3
C_3S	$(1.8\pm0.2)\times10^{11}$	33.6 ± 7.0	$(5.7\pm1.0)\times10^{11}$	15.1 ± 1.4	$(1.8\pm0.4)\times10^{13}$	7.4 ± 0.8
$C_3{}^{34}S$	$< 9.2\times10^{10}$ [b]	33.6[c]	$< 5.2\times10^{10}$ [b]	15.1[c]	$(1.4\pm0.7)\times10^{12}$	2.8 ± 0.9
OCS	$< 8.4\times10^{11}$ [b]	10.0[c]	$(3.7\pm0.3)\times10^{13}$	37.0 ± 2.7	$(3.8\pm0.5)\times10^{13}$	7.0 ± 0.8
			$(3.6\pm0.6)\times10^{13}$	126.0 ± 32.5		
$OC^{34}S$	$< 5.9\times10^{11}$ [b]	10.0[c]	$(5.7\pm0.5)\times10^{12}$	82.9 ± 11.0	-	-
$OC^{33}S$	$< 1.8\times10^{12}$ [b]	10.0[c]	$< 3.0\times10^{12}$ [b]	82.9[c]	-	-
HCS^+	$(3.1\pm1.5)\times10^{11}$	10.0[c]	$(7.1\pm1.5)\times10^{11}$	14.0 ± 1.7	$(5.0\pm2.0)\times10^{12}$	3.8 ± 0.4
$HC^{34}S^+$	$< 1.2\times10^{11}$ [b]	10.0[c]	$< 1.4\times10^{11}$ [b]	14.0[c]	$(8.0\pm2.0)\times10^{11}$	6.0 ± 1.0
SO	$(4.9\pm0.8)\times10^{12}$	7.7 ± 0.5	$(1.0\pm0.2)\times10^{14}$	12.1 ± 0.6	$(1.8\pm0.6)\times10^{13}$	7.2 ± 0.1
^{34}SO	$(2.6\pm1.3)\times10^{11}$	7.7[c]	$(7.2\pm1.4)\times10^{12}$	9.8 ± 0.5	$(2.5\pm1.3)\times10^{12}$	-
$S^{18}O$	$< 2.1\times10^{11}$ [b]	7.7[c]	$(1.2\pm0.6)\times10^{12}$	9.1 ± 2.4	-	-
H_2CS	$(9.3\pm4.6)\times10^{11}$	7.0 ± 3.5	$(1.1\pm0.2)\times10^{13}$	19.2 ± 1.4	p- $(6.0\pm2.0)\times10^{12}$	p- 5.4 ± 0.2
			$(6.9\pm3.4)\times10^{12}$	62.1 ± 31.1	o- $(1.6\pm0.7)\times10^{13}$	o- 4.5 ± 0.5
SO_2	$(9.3\pm4.7)\times10^{11}$	10.0[c]	$(1.2\pm0.3)\times10^{13}$	10.1 ± 1.0	$(4.7\pm2.4)\times10^{12}$	-
			$(1.1\pm0.8)\times10^{13}$	17.4 ± 3.4		
$^{34}SO_2$	$< 3.8\times10^{11}$ [b]	10.0[c]	$(1.1\pm0.6)\times10^{12}$	11.6 ± 4.9	-	-
NS	$< 1.5\times10^{12}$ [b]	10.0[c]	$(5.4\pm0.7)\times10^{12}$	10.1 ± 0.4	$(1.3\pm0.7)\times10^{12}$	-
NS^+	$< 5.1\times10^{10}$ [b]	10.0[c]	$(7.8\pm3.9)\times10^{10}$	6.9 ± 3.5	-	-
H_2S	$(2.0\pm1.0)\times10^{12}$	10.0[c]	$(3.4\pm1.7)\times10^{13}$	43.6 ± 21.8	$(6.5\pm3.3)\times10^{13}$	-
$H_2{}^{34}S$	$< 5.6\times10^{11}$ [b]	10.0[c]	$(1.0\pm0.5)\times10^{13}$	47.8 ± 23.9	$(1.1\pm0.6)\times10^{12}$	-
HSCN	$< 6.0\times10^{10}$ [b]	10.0[c]	$(1.5\pm0.7)\times10^{11}$	37.0[c]	$(1.0\pm0.5)\times10^{12}$	-
HNCS	$< 1.6\times10^{11}$ [b]	10.0[c]	$< 7.1\times10^{11}$ [b]	37.0[c]	$(4.7\pm2.4)\times10^{12}$	-
$C^{17}O$	$(7.9\pm4.0)\times10^{13}$	10.0[c]	$(1.1\pm0.5)\times10^{15}$	16.2[c]	$(7.3\pm3.7)\times10^{14}$	10.0[c]
$C^{18}O$	-[d]	-	$(3.0\pm1.5)\times10^{15}$	16.2 ± 8.1	$(1.8\pm0.9)\times10^{15}$	10.0[c]
CH_3OH	$(1.5\pm0.6)\times10^{13}$	5.3 ± 0.7	$(1.0\pm0.4)\times10^{14}$	9.8 ± 1.6	$(2.1\pm0.7)\times10^{13}$	6.9 ± 0.8
			$(1.2\pm0.6)\times10^{14}$	34.6 ± 9.0	$(1.6\pm0.5)\times10^{13}$	35.8 ± 7.8
H_2CO	$(1.1\pm0.4)\times10^{13}$	24.1 ± 12.8	p- $(1.4\pm0.3)\times10^{13}$	p- 10.5 ± 1.9	$(1.3\pm0.2)\times10^{13}$	21.4 ± 4.2
			p- $(3.2\pm0.1)\times10^{13}$	p- 66.0 ± 2.9		
			o- $(3.2\pm0.2)\times10^{13}$	o- 10.1 ± 0.3		
			o- $(3.8\pm1.9)\times10^{13}$	o- 36.8 ± 18.4		

---

[a] Results for S-bearing molecules taken from [5].

[b] Column density upper limit for the undetected species.

[c] Rotational temperature has been fixed.

[d] No transitions fall under the spectral range.

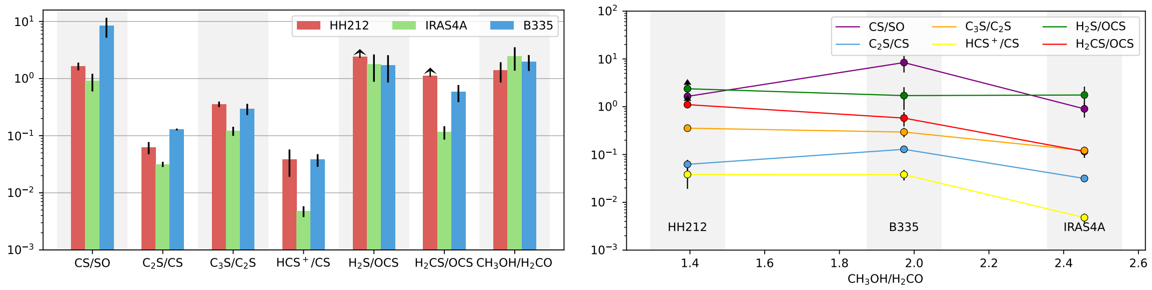

Figure 2: Left: abundance ratios of molecules in HH 212, IRAS4A and B 335. Right: comparison of CH_3OH/H_2CO to other abundance ratios.

3.2 Abundances & Ratios

After computing the isotopologue ratios of all species and objects, we observe in Fig. 1 that some $^{34}S/^{32}S$ ratios have a higher value than the solar isotopic ratio. In those cases, we are going to assume that the corresponding molecule is optically thick. We then calculate the abundances using a $C^{18}O$ abundance of $1.7 \cdot 10^{-7}$ [13] and the column densities in Table 2. When one species had two $T_{\rm rot}$ we used the N associated with the colder temperature, as to focus on the envelope of each object. For the optically thick species, we obtain the abundance from their isotopologues. Results are in Fig. 1 and, as seen in the figure, the main differences are found between B 335 and the other two protostars, particularly in CS, C_2S, C_3S, HCS^+, and their isotopologues. In B 335 the CS abundance is at least 5 times higher than in the other two, while for C_2S and C_3S this factor becomes of at least 20. In addition, the HCS^+ abundance is at least 10 times higher in this object as well. We also note that OCS, one of the most abundant S-bearing molecules in IRAS4A and B 335, was not detected in HH 212.

In Fig. 2 we plot some interesting abundance ratios of each source, showing more fundamental differences between these objects. It is evident that the CS/SO ratio is highest in B 335: 10 times larger than in IRAS4A and 5 times larger than in HH 212. When discussing the C_2S/CS, C_3S/C_2S and HCS^+/CS ratios, IRAS4A has the lowest: the HCS^+/CS ratio is 8 times smaller, and the C_2S/CS and C_3S/C_2S ratios are 3 times smaller than the other two. Furthermore, when comparing the CH_3OH/H_2CO ratio against the others (also in Fig. 2), it seems that it is inversely correlated to the ratios HCS^+/CS, H_2CS/OCS and C_3S/C_2S.

Adding a few more results of other prestellar and protostellar objects, we see in Fig. 3 that the SO/CS, SO_2/C_2S and HCS^+/CS ratios are potential tracers of the evolution of young protostars: SO/CS and SO_2/C_2S increase with age while HCS^+/CS decreases with age, as it was already proposed in [5]. These assessments are key to understand which part of their chemistry changes due to the surrounding environment and the evolutionary stage.

Acknowledgments

This work is supported by ERC grant SUL4LIFE, GA No. 101096293, funded by the European Union. Views and opinions expressed are however those of the authors only and do not necessarily reflect those

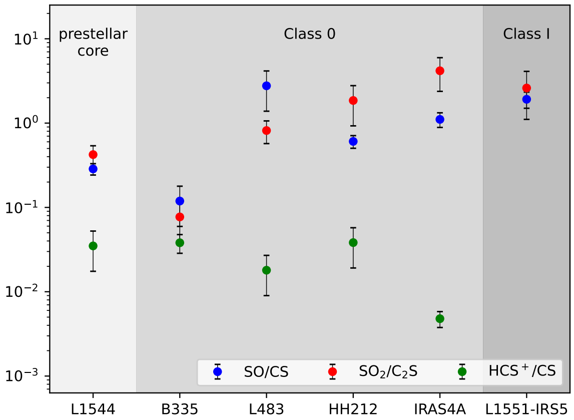

Figure 3: SO/CS, SO_2/C_2S and HCS^+/CS ratios for different prestellar and protostellar sources. Data for L1544 taken from [14], B 335 from [5], L483 from [1] and L1551-IRS5 from [10].

of the European Union or the European Research Council Executive Agency. Neither the European Union nor the granting authority can be held responsible for them.

References

[1] Agúndez, M., Marcelino, N., Cernicharo, J., Roueff, E., & Tafalla, M. 2019, A&A, 625, A147

[2] Anders, E. & Grevesse, N. 1989, Geochimica et Cosmochimica acta, 53, 197

[3] Ceccarelli, C. 2004, in ASP Conf. Ser., 323, Star Formation in the Interstellar Medium: In Honor of David Hollenbach, eds. D. Johnstone, F. C. Adams, D. N. C. Lin, D. A. Neufeeld, & E. C. Ostriker, 195

[4] Ceccarelli, L., Valotto, C., Lambas, D. G., & Padilla, N. 2007, in ASP Conf. Ser., 379, Cosmic Frontiers, eds. N. Metcalfe, & T. Shanks, 287

[5] Esplugues, G., Rodríguez-Baras, M., San Andrés, D., et al. 2023, A&A, 678, A199

[6] Goldsmith, P. F. & Langer, W. D. 1999, ApJ, 517, 209

[7] Herbst, E., & van Dishoeck, E. F. 2009, ARA&A, 47, 427

[8] Lefloch, B., Bachiller, R., Ceccarelli, C., et al. 2018, MNRAS, 477, 4792

[9] Leustek, T. 2002, Arabidopsis Book, 1, e0017

[10] Marchand, P., Coutens, A., Scigliuto, J., et al. 2024, A&A, 687, A195

[11] Shingledecker, C. N., Lamberts, T., Laas, J. C., et al. 2020, ApJ, 888, 52

[12] Tieftrunk, A., Pineau des Forets, G., Schilke, P., & Walmsley, C. M. 1994, A&A, 289, 579

[13] Treviño-Morales, S., Fuente, A., Sánchez-Monge, Á., et al. 2019, A&A, 629, A81

[14] Vastel, C., Quénard, D., Le Gal, R., et al. 2018, MNRAS, 478, 5514